Electronic Supplementary Material (ESI) for Energy Advances.

Supporting Information

Hierarchically porous N-doped carbon nanosheets with atomically dispersed Fe/Co dual-metallic sites for efficient and robust oxygen electrocatalysis in Zn-air batteries

Zheng-Qi Liu[a], Fei-Xiang Ma[a]*, Yu-Xuan Xiong[a], Meng-Tian Zhang[a], Liang Zhen[a, b], Cheng-Yan Xu[a, b]*

[a] Sauvage Laboratory for Smart Materials, School of Materials Science and Engineering, Harbin Institute of Technology (Shenzhen), Shenzhen 518055, China

[b] State Key Laboratory of Advanced Welding and Joining, Harbin Institute of Technology, Harbin 150001, China

Email: mafeixiang@hit.edu.cn; cy_xu@hit.edu.cn

Materials

Commercial Pt/C (20 wt% Pt) catalyst was bought from Shanghai Hesen Electric Co., Ltd. (CHN). Nafion solution (5 wt%) was purchased from DuPont (USA). Polyvinylpyrrolidone (PVP, K30), Ferric Nitrate Nonahydrate ($Fe(NO_3)_3 \cdot 9H_2O$, Analytical reagent, 98%), Cobalt(II) Nitrate Hexahydrate($Co(NO_3)_2 \cdot 6H_2O$, Analytical reagent, 99%), Nickel(II) chloride hexahydrate($NiCl_2 \cdot 6H_2O$, Analytical reagent, 99%), Hydrochloric acid (HCl, Analytical reagent, 37%), Manganese(II) Nitrate Tetrahydrate($Mn(NO_3)_2 \cdot 4H_2O$, Analytical reagent, ≥98%) were bought from Adamas-beta(CHN). Dicyandiamide ($C_2H_4N_4$, Analytical reagent, 99%), Potassium hydroxide (KOH, Analytical reagent, 90%), Copper chloride dihydrate ($CuCl_2 \cdot 2H_2O$, Analytical reagent, ≥99%), Iron(III) chloride hexahydrate($FeCl_3 \cdot 6H_2O$, Analytical reagent, ≥99%) , Isopropanol ($(CH_3)_2CHOH$, Analytical reagent, ≥99.7%) and Ethanol (C_2H_5OH, Analytical reagent, ≥99.7%) were purchased from General-Reagent (CHN). All of the chemicals were used directly without further purification. Deionized water was used for all experiments.

Electrochemical measurements

Electrochemical measurements were carried out in a three-electrode system on a CHI 760E electrochemical workstation (Shanghai Chenhua, China) coupled with a RRDE-3A (Rotating Ring Disk Electrode Apparatus Ver.2.0 ALS Co., Ltd Japan) in 0.1 M KOH electrolyte. A glassy carbon (GC) RDE of 3 mm in diameter was served as the working electrode, a saturated calomel electrode (SCE) and a carbon rod were used as reference and counter electrode, respectively. All electrode potential in this work were converted into reversible hydrogen electrode potentials (RHE), using the calibration equation ($E_{RHE} = E_{SCE} + 0.244 + 0.059pH$).

Cyclic voltammetry (CV) measurement. Before the test, the electrolyte was saturated with oxygen by bubbling O_2 20 min to ensure its oxygen saturation state. The working electrode was

electroactivated by conducting 30 voltammetric cycles at 50 mV s^{-1} with the potential ranging from 0.2 to 1.1 V vs. RHE in order to get stable curves. A flow of O_2 was maintained in the electrolyte during the recording of CVs.

Rotating disk electrode (RDE) measurement. The working electrode was scanned cathodically at a rate of 5 mV s^{-1} and a potential range of 0.2 to 1.1 V vs. RHE with varying rotating speed from 900 rpm to 2500 rpm. Koutecky–Levich (K-L) plots were analyzed at various electrode potentials. The slopes of their best linear fit lines were used to calculate the number of electrons transferred number (n) and kinetic current density (J_K) on the basis of the K-L equation.

$$1/J = 1/J_K + 1/J_L = 1/J_K + 1/(B\omega^{1/2})$$

$$B = 0.62nFC_0D_0^{2/3}V^{-1/6}$$

$$J_K=nFkC_0$$

J ----- current density,

J_K ----- kinetic current density

J_L ----- limiting current density

ω ----- Angular Velocity

n ----- Total Electron Transfer Number

F ----- Faraday constant (96485 C mol^{-1}),

D_0 ----- Diffusion Coefficient of O_2 (1.9×10^{-5} $cm^2 \cdot s^{-1}$)

C_0 ----- Bulk concentration of O_2 (1.2×10^{-6} mol cm^{-3}),

v ----- Kinematic viscosity of the electrolyte (0.01 cm^2 s^{-1}),

k ----- Electron-transfer rate constant.

For the Tafel plot, the kinetic current density (rotating speed of 1600 rpm) for assessing the ORR

kinetics was calculated from the mass-transport correction of the RDE data by:

$J_K = J^*J_L/(J_L-J)$

Turn-Over frequency (TOF) of the Fe/Co-N-C, Fe-N-C and Pt/C were calculated based on the mole number of active Fe-Co dual sites, Fe single sites and Pt single sites, respectively. The TOF values were calculated using the equation:

$TOF=I/(4*m*F)$

Where I is the measured current at 0.85 V, 4 is the number of electrons transferred during O_2 reduction, m is the mole number of active Fe-Co dual sites, Fe single sites and Pt single sites on the electrode, and F is the Faraday constant (F = 96,485 C mol^{-1}).

Rotating ring-disk electrode (RRDE) measurement. H_2O_2 produced at the disk electrode can be detected by the ring electrode. The disk electrode was scanned cathodically at a rate of 5 mV s^{-1} and the ring potential was constant at 1.3 V vs. RHE. The hydrogen peroxide yield [H_2O_2 (%)] and the electron transfer number (n) were determined by the followed equations:

$H_2O_2(\%)=200*(I_R/N)/(I_R/N+I_D)$

$n = 4\times I_D/(I_R/N+I_D)$

I_D ----- Disk Current

I_R ----- Ring Current

N ----- Ring Collection Coefficient (N=0.4)

The electrochemical durability of the catalysts with respect to commercial Pt/C by using chronoamperometric (CA) measurements at 0.51 V (vs. RHE) for 12 hours in O_2-saturated 0.1 M KOH at a rotation rate of 1600 rpm.

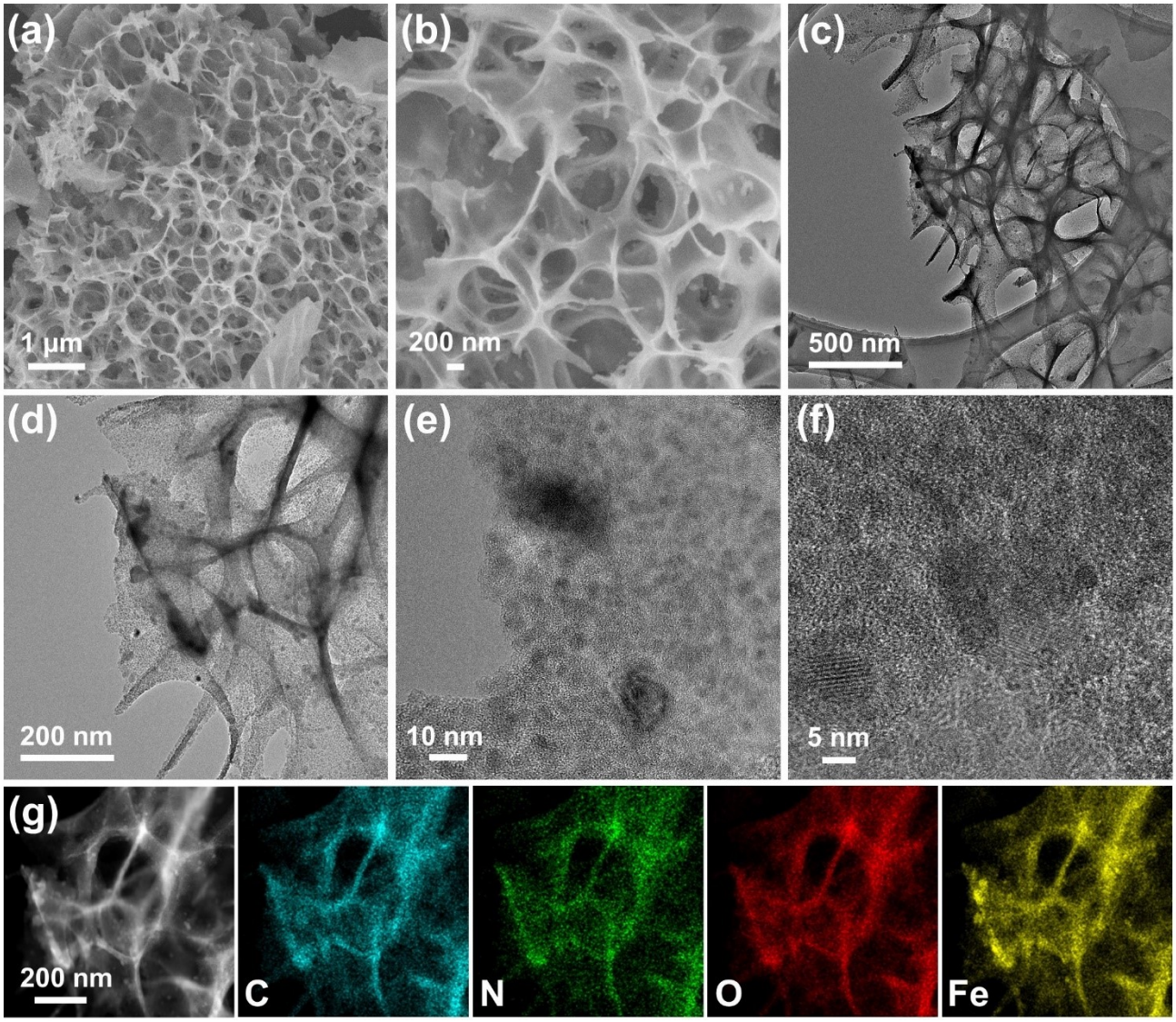

Figure S1 Microstructure characterization of as-prepared carbon nanosheets uniformly decorated with iron nanoparticles. (a, b) SEM, (c-e) TEM, (f) HRTEM images and (g) elemental mapping of C, N, O and Fe.

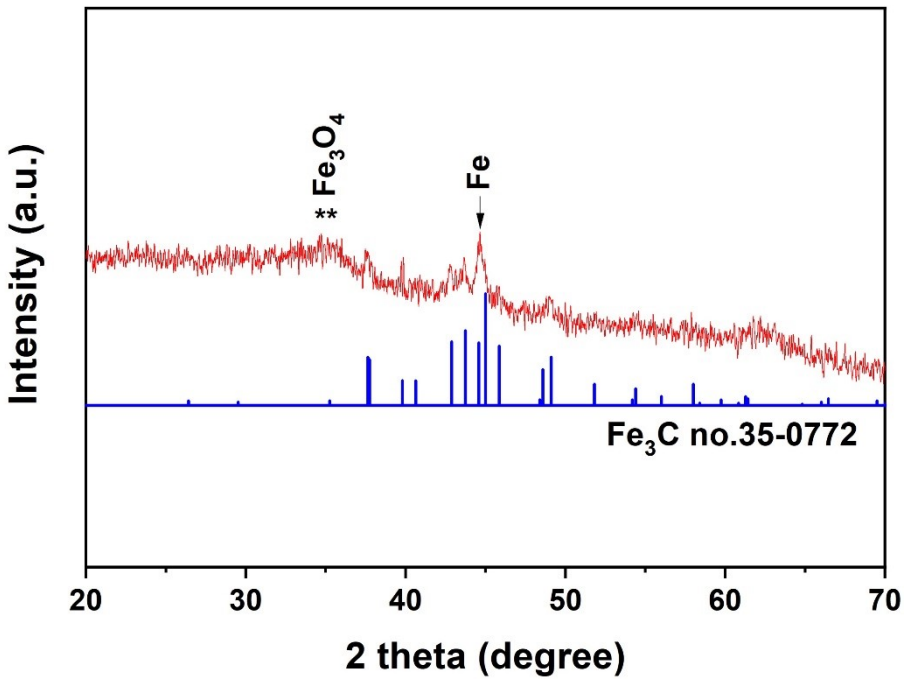

Figure S2 XRD patterns of carbon nanosheets uniformly decorated with iron nanoparticles.

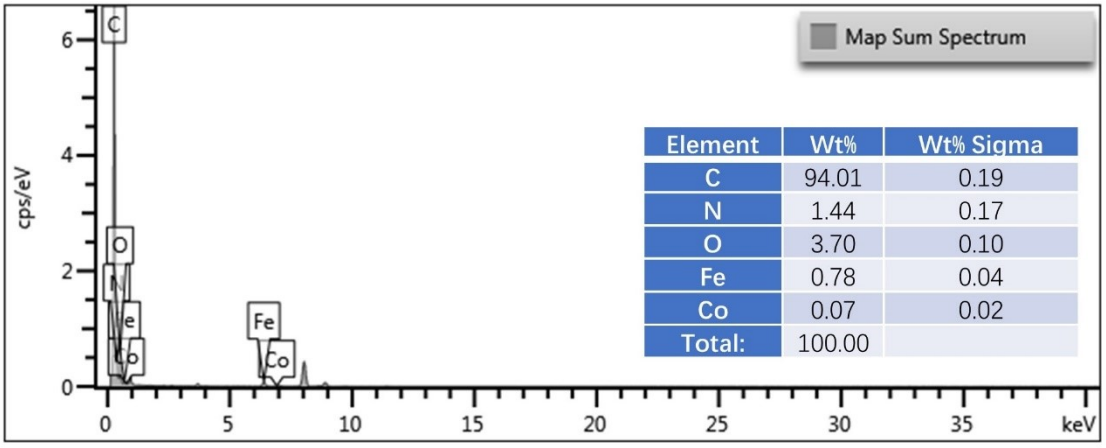

Element	Wt%	Wt% Sigma
C	94.01	0.19
N	1.44	0.17
O	3.70	0.10
Fe	0.78	0.04
Co	0.07	0.02
Total:	100.00	

Figure S3 The elements contents for Fe/Co-N-C

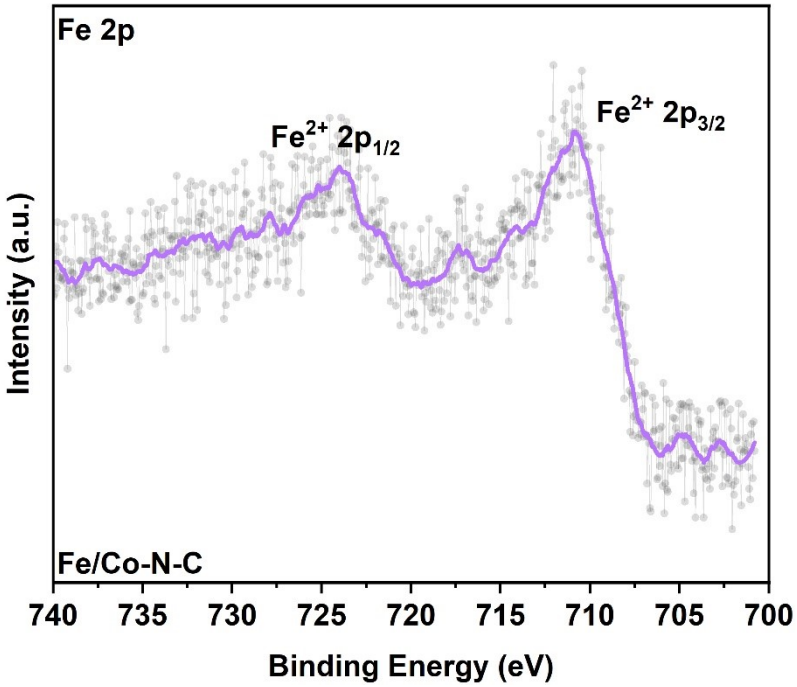

Figure S4. XPS Fe 2p spectra of Fe/Co-N-C.

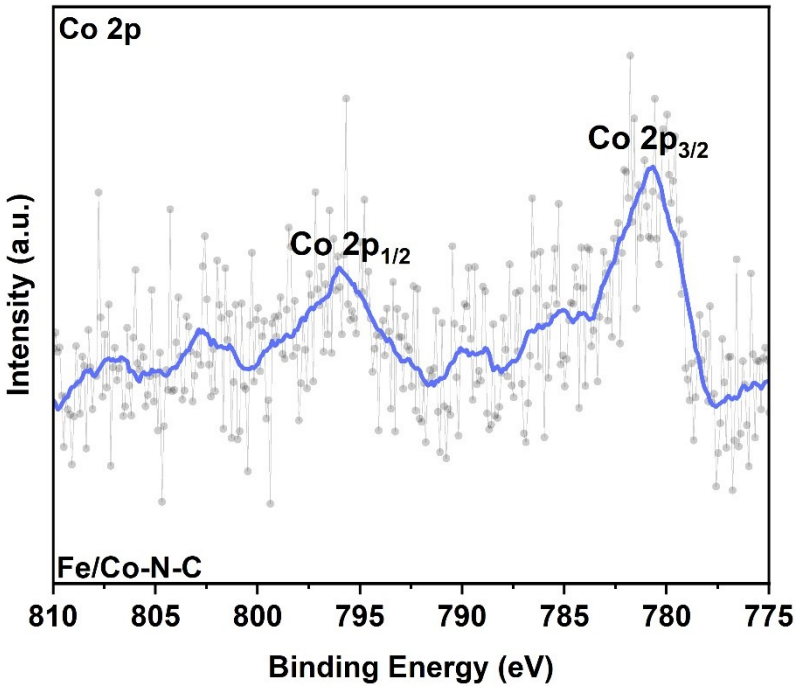

Figure S5. XPS Co 2p spectra of Fe/Co-N-C.

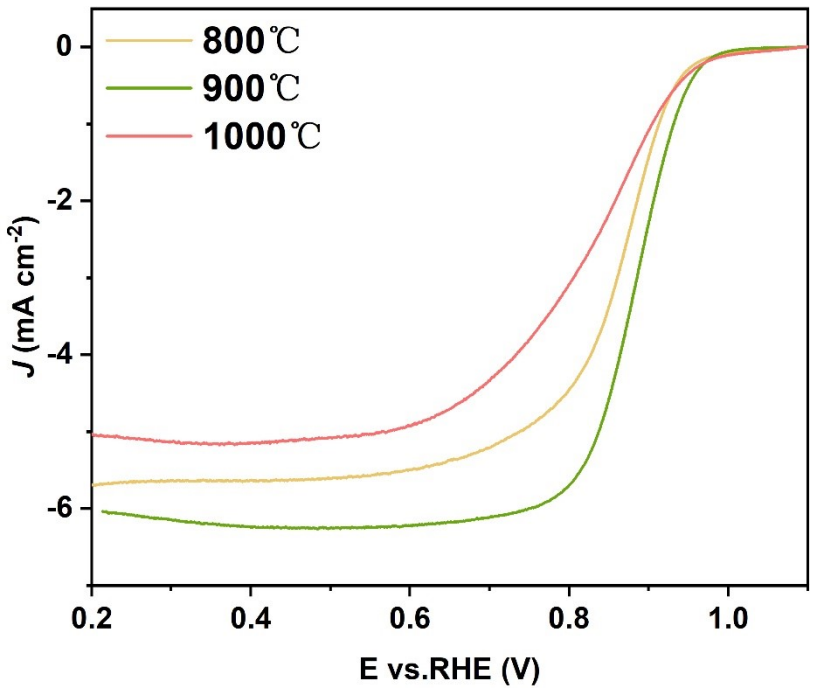

Figure S6. ORR polarization curves of Fe/Co-N-C at different annealing temperatures.

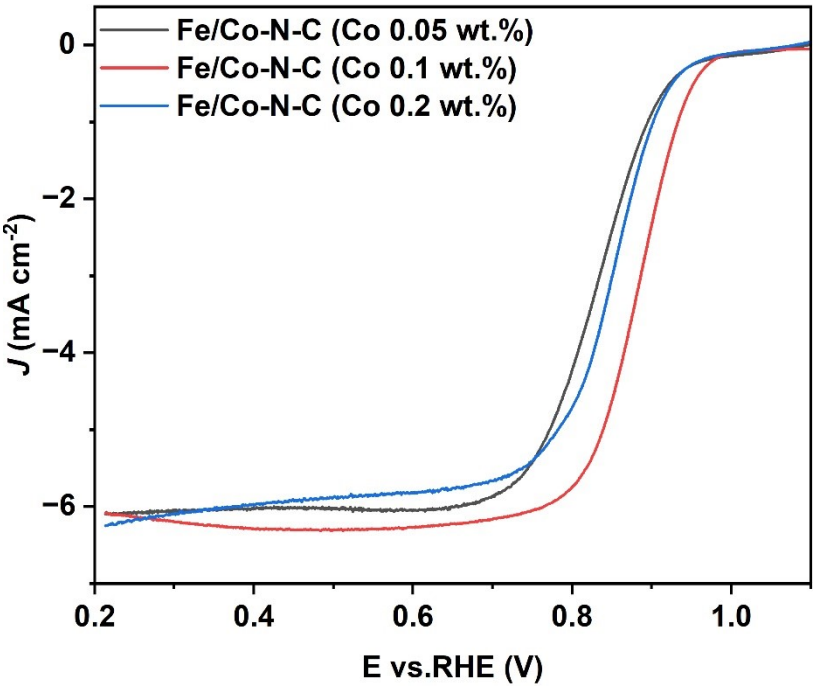

Figure S7. ORR polarization curves of Fe/Co-N-C with different cobalt content at 900 °C.

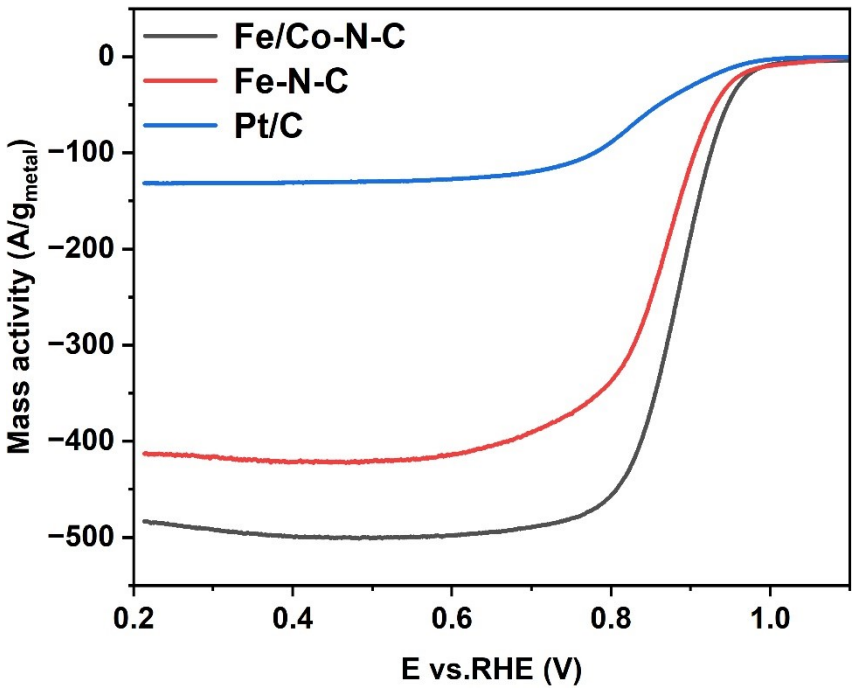

Figure S8. Mass activity comparison of Fe/Co-N-C, Fe-N-C and commercial Pt/C.

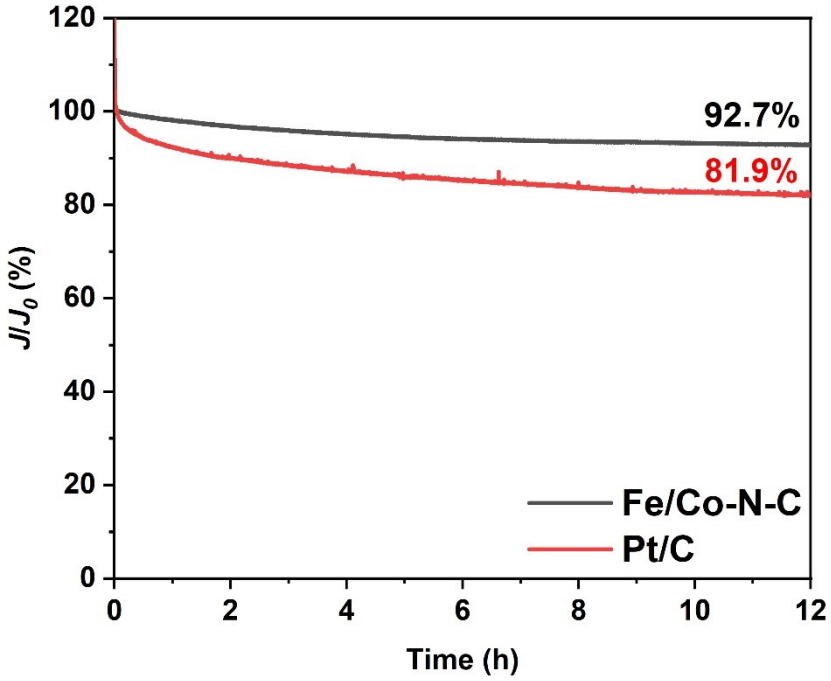

Figure S9. Durability comparison between Fe/Co-N-C and commercial Pt/C tested at 0.5 V vs RHE.

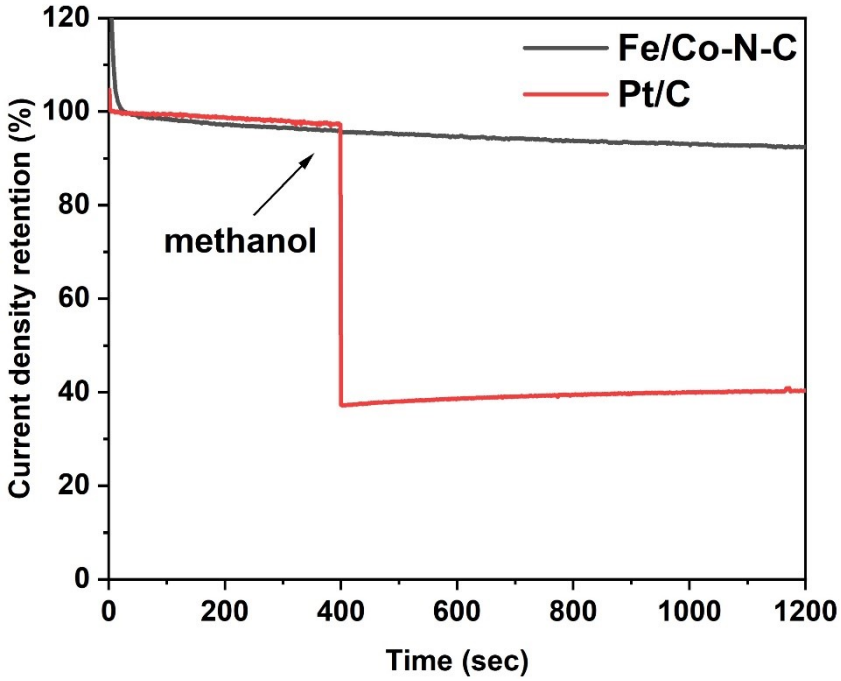

Figure S10. Current density retention curves of Fe/Co-N-C and Pt/C at 0.5 V in 0.1 M KOH with re-addition of 1 M methanol.

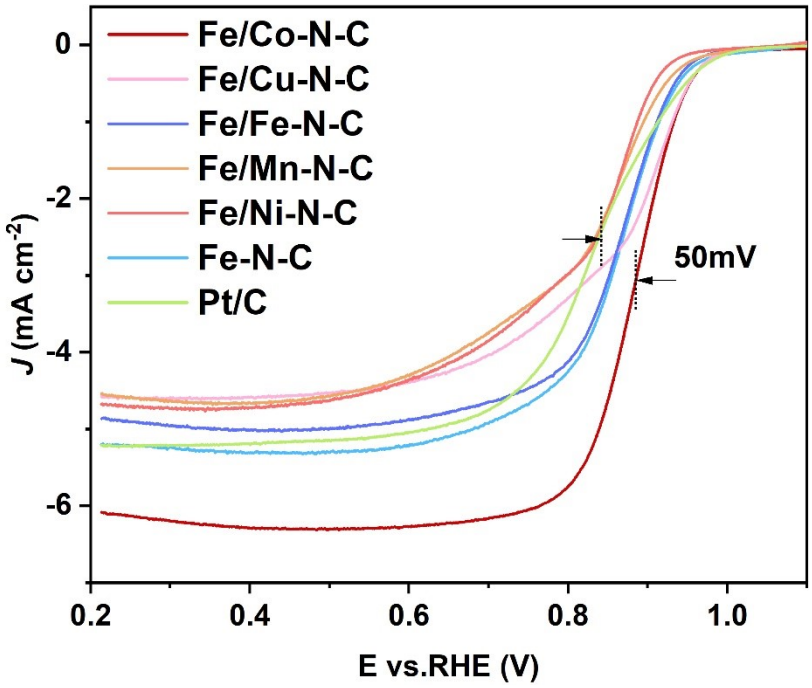

Figure S11. ORR polarization curves for Fe/Co-N-C and Fe-N-C compared with adsorb other metals.

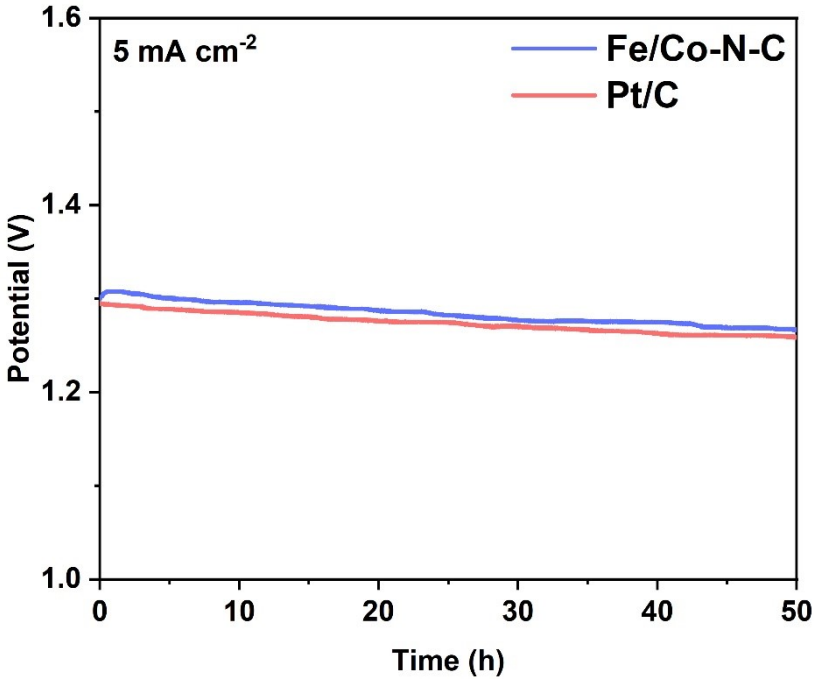

Figure S12. Galvanostatic discharge curves of zinc-air batteries at a current density of 5 mA·cm^{-2}.

Table S1. Comparison of ORR catalytic performances in alkaline solution between Fe/Co-N-C series catalysts and other previously reported catalysts.

Catalyst	$E_{1/2}$ (V)	J_d (mA cm^{-2}) @0.5 V	Reference
Fe/Co-N-C	0.88	6.2	This work
Fe,Co,N-CNP(0.3)	0.875	5.355	[1]
$Fe_{1.2}Co$@NC/NCNTs	0.82	5.5	[2]
Fe_1Co_7-N-C	0.816	4.86	[3]
Fe,Co-NPC-800	0.855	6.32	[4]
Fe-Co-N-OMC (1:1)	0.83	5.7	[5]
FeCo-N-HCN	0.86	5.3	[6]
Fe_1Co_1-CNF	0.87	5.4	[7]
Fe-Co(0.4)/N-rGO-AL	0.84	5.2	[8]
Co/Fe-NC	0.847	5.82	[9]
$Fe_3C/CoFe_2O_4$@CNFs-1.5	0.84	5.9	[10]

References

[1] Z. Hu, Z. Guo, Z. Zhang, M. Dou, F. Wang, Bimetal Zeolitic Imidazolite Framework-Derived Iron-, Cobalt- and Nitrogen-Codoped Carbon Nanopolyhedra Electrocatalyst for Efficient Oxygen Reduction, ACS Appl Mater Interfaces 10(15) (2018) 12651-12658.

[2] S. Li, W. Chen, H. Pan, Y. Cao, Z. Jiang, X. Tian, X. Hao, T. Maiyalagan, Z.-J. Jiang, FeCo Alloy Nanoparticles Coated by an Ultrathin N-Doped Carbon Layer and Encapsulated in Carbon Nanotubes as a Highly Efficient Bifunctional Air Electrode for Rechargeable Zn-Air Batteries, ACS Sustainable Chemistry & Engineering 7(9) (2019) 8530-8541.

[3] Z.Y. Zu, J.L. Mi, B. Wu, L. Liu, Fe/Co Containing N-Doped Hierarchical Porous Carbon Microcuboids and Microcylinders as Efficient Catalysts for Oxygen Reduction Reaction, ChemCatChem 12(22) (2020) 5780-5788.

[4] X. Jia, W. Gu, S. Zhang, E. Wang, In Situ Formation of Hierarchical Porous Fe,Co−N-Doped Carbon as a Highly Efficient Electrocatalyst for Oxygen Reduction, ChemElectroChem 4(8) (2017) 2005-2011.

[5] W. Ran, J. Dong, T. Sun, J. Chen, L. Xu, Iron, Cobalt, and Nitrogen Tri-Doped Ordered Mesoporous Carbon as a Highly Efficient Electrocatalyst for Oxygen Reduction Reaction, ChemistrySelect 4(26) (2019) 7728-7733.

[6] H. Li, Y. Wen, M. Jiang, Y. Yao, H. Zhou, Z. Huang, J. Li, S. Jiao, Y. Kuang, S. Luo, Understanding of Neighboring Fe-N4-C and Co-N4-C Dual Active Centers for Oxygen Reduction Reaction, Advanced Functional Materials 31(22) (2021).

[7] Y. Wang, Z. Li, P. Zhang, Y. Pan, Y. Zhang, Q. Cai, S.R.P. Silva, J. Liu, G. Zhang, X. Sun, Z. Yan, Flexible carbon nanofiber film with diatomic Fe-Co sites for efficient oxygen reduction and evolution reactions in wearable zinc-air batteries, Nano Energy 87 (2021).

[8] Q. Niu, J. Guo, Y. Tang, X. Guo, J. Nie, G. Ma, Sandwich-type Bimetal-Organic Frameworks/Graphene Oxide Derived Porous Nanosheets doped Fe/Co-N Active Sites for Oxygen Reduction Reaction, Electrochimica Acta 255 (2017) 72-82.

[9] Y. Wang, Y. Pan, L. Zhu, H. Yu, B. Duan, R. Wang, Z. Zhang, S. Qiu, Solvent-free assembly of Co/Fe-containing MOFs derived N-doped mesoporous carbon nanosheets for ORR and HER, Carbon 146 (2019) 671-679.

[10] Y. Sun, Y. Li, S. You, X. Li, Y. Zhang, Z. Cai, M. Liu, N. Ren, J. Zou, Fe3C/CoFe2O4 nanoparticles wrapped in one-dimensional MIL-53(Fe)-derived carbon nanofibers as efficient dual-function oxygen catalysts, Chemical Engineering Journal 424 (2021) 130460.